

RESONANCE ON TRANSFORMERS EXCITED BY SQUARE WAVES AND EXPLANATION OF THE HIGH VOLTAGE ON TESLA TRANSFORMER

E. M. M. Costa

Colegiado de Engenharia Elétrica — CENEL
Universidade Federal do Vale do São Francisco — UNIVASF
Av. Antônio Carlos Magalhães, 510, Juazeiro, BA, Brazil

Abstract—This paper presents an analysis about resonance on coupled systems when excited by square waves, generated through experiments using planar and ring coils. Because of the phenomenon described by its transfer function, a sum of responses appear when the square wave frequency increases, which causes a resonance response with high voltage, in several cases, greater than common turn ratio of the transformer. With parallel capacitances inserted on output, the resonance frequency reduction and change of gain is observed. Due to this effect, explanation of how output of Tesla transformer presents high voltage which is shown and strategies to reach the maximal value on output are proposed.

1. INTRODUCTION

In several researches about resonance, studies have been developed considering effects of impedances on RLC circuits [1–4]. Others analyze disks [5, 6], as well transformers, where excitation is sinusoidal [7–12] or, in some cases, square waves [13, 14]. Naturally, studies about excitation of circuits by square wave is generally applied to power electronics [15, 16], pulse waves [17–22] or pulse transformers [23–28]. In these cases, we find in literature researches applied to Tesla transformer [29–32] where resonance phenomena are hardly described, being seen as a doubly resonant effect.

As known, Tesla transformer presents a phenomenon of high voltage obtained through resonance of LC circuit, where the inductor L is a secondary of transformer with primary excited by a pulsed voltage (square wave) above 10 kV. In Tesla transformer the output may be in

Corresponding author: E. M. M. Costa (eduard.montgomery@univasf.edu.br).

order above 500 kV [29–32]. However, in literature little is found about how this effect occurs.

When analyzing pulsed systems, i.e., transformers excited by square waves, some important results are presented, which are analyzed in several ways, through parasitic capacitances [33–37], transfer function [38] or resonance due parasitic capacitances and self and mutual inductances [39]. In these cases, we found air core transformers built with planar coils and inner ring coils, although many researches in the literature on planar coils [40–44] are found in microcircuits [45–51].

However, these results show important information to explain the phenomenon of resonance and high voltage output Tesla transformer, specially when these systems engage parallel capacitances in secondary (output). Consequently, due to this insertion, the resonance frequency is lower than system without these capacitances, and output voltage may be higher. These effects generate high gains that is observed as the sum of system response to input step voltage (each rise and fall of the square wave appear as step voltage positive and negative, respectively) added with a proportional gain due to turn ratio of the transformer (specially visible in cases when the turn ratio is greater than one, if the parameters of the coils are satisfied, as resistances, inductances and capacitances) [39]. Consequently, these effects are presented as resonance in these systems, and their occurrence generates high voltage on Tesla transformer, as will be shown in this paper.

Considering this information, this paper shows the experimental work that these results are based. In this way, this paper is presented as follows: in Section 2, basic data of equipments and experiments are presented; in Section 3 we show basic results about obtained data and realized experiments, with the transfer function of the system and the formulation of the resonance; in Section 4 the information about insertions of parallel capacitances on output of the system and their effects is presented; in Section 5 we show behavior of Tesla transformer and comparisons with obtained results; in Section 6 we present conclusions of this work.

2. BASIC DATA

Based on data and experiments described in [33] and performing other experiments with other coils and inserting parallel capacitances to the output, we have analyzed the observed effects to determine the phenomena of high-voltage Tesla transformer.

The equipment used included a digital storage oscilloscope Agilent Technologies DSO3202A with passive probe N2862A (input resistance = 10 M Ω and input capacitance \simeq 12 pF), a function

generator Rigol DG2021A and a digital multimeter Agilent Technologies U1252A.

The coils utilized to obtain the results were:

- 7 planar coils with turn number: 10, 20, 50, 200, 500 and 1600;
- 10 ring coils with turn number: 2, 5, 7, 9, 10, 12, 15, 20, 30 and 50;
- 6 capacitors with capacitances: 4.7 pF, 10 pF, 56 pF, 155 pF, 253 pF and 1443 pF, whose values were measured with cited digital multimeter.

Data of the realized experiments were obtained considering the transformer (systems) being built by planar coil inner ring coils. All experiments were realized exciting primary coil system and observing the induced *emf* (response) on secondary. The input square wave frequencies ranged from 1 kHz to 25 MHz, with voltage 5 V peak to peak. In resonance, data were obtained without capacitances and insertion of output parallel capacitance, where in these cases, the input square wave voltage had voltage variation from 1 to 10 V.

The coils used, as well as other information on structure and equivalent circuit, may be seen in [33, 38].

3. INITIAL EXPERIMENTS AND RESULTS

As we see in Costa [33], when exciting the primary of this system by a square wave, and observing the response on secondary, effects of parasitic capacitances on coils are observed. These effects may be determined by transfer function of the system [38], where in higher frequencies the sum of responses generates resonance on output [39]. In this section, some results are presented in summarized way.

The system response was obtained by graphs in oscilloscope in all the experiments, and some of these results are shown in Fig. 1, given by:

$$v_0 = A \left[\sin(\omega_1 t) \sin(\omega_2 t) e^{-bt} + c \right] e^{-dt} \quad (1)$$

where this equation was obtained from graph in configuration 200 turns planar coil *vs* 10 turns ring coil, being valid for all configurations (variations on self inductances, mutual inductance, resistances and parasitic capacitances changes ω_1 , ω_2 , and exponential drops b and d).

Considering parameters $y_1 = (\omega_1 + \omega_2)^2$, $y_2 = (\omega_1 - \omega_2)^2$ and $x = b + d$, we have the transfer function of the system given by [38]:

$$G(s) = \frac{z_5 s^5 + z_4 s^4 + z_3 s^3 + z_2 s^2 + z_1 s}{s^5 + p_4 s^4 + p_3 s^3 + p_2 s^2 + p_1 s + p_0} \quad (2)$$

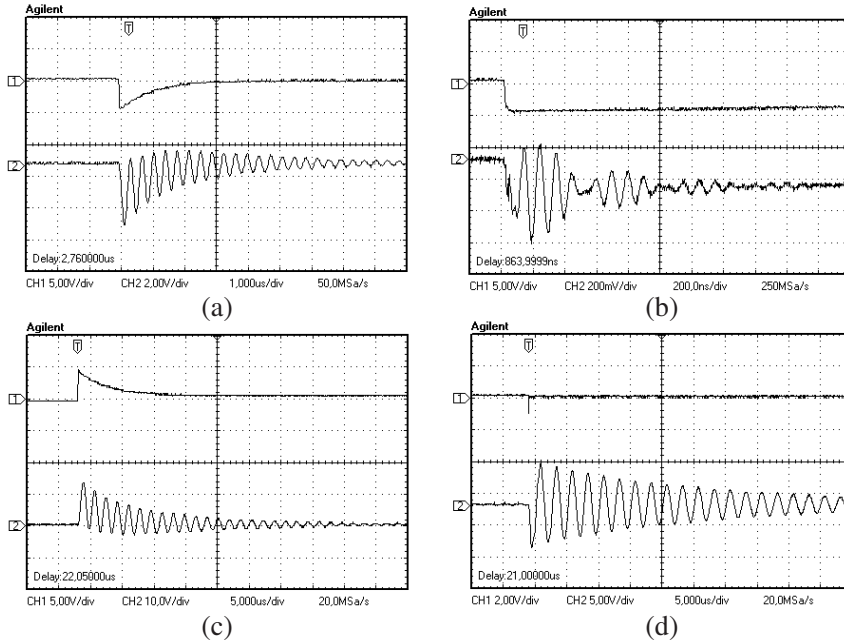


Figure 1. Some responses of the system for low frequencies (or step voltage): Direct system (a) 50 turns planar coil *vs* 30 turns ring coil; (b) 200 turns planar coil *vs* 9 turns ring coil; and inverted system (c) 50 turns ring coil *vs* 500 turns planar coil; (d) 2 turns ring coil *vs* 1600 turns planar coil.

where $z_5 = c$, $z_4 = 4xc$, $z_3 = (6x^2 + y_2 + y_1)c + 2(y_2 - y_1)a$, $z_2 = (4x^3 + 2x(y_2 + y_1))c + 2(y_2 - y_1)(x + d)a$, $z_1 = (x^4 + x^2(y_2 + y_1) + y_2y_1)c + 2(y_2 - y_1)xda$, and $p_4 = 4x + d$, $p_3 = 6x^2 + y_2 + y_1 + 4xd$, $p_2 = 4x^3 + 6x^2d + (2x + d)(y_2 + y_1)$, $p_1 = x^4 + 4x^3d + (2xd + x^2)(y_2 + y_1) + y_2y_1$ and $p_0 = (x^4 + x^2(y_2 + y_1) + y_2y_1)d$.

When the frequency of the square wave is increased, sum of responses that varies output voltage occurs, as shown in Fig. 2, in configuration 200 planar coil *vs* 30 ring coil (direct system) on sequential frequencies 167 kHz, 178 kHz and 191 kHz, and in configuration 15 ring coil *vs* 500 planar coil (inverted system) on sequential frequencies 80 kHz, 90 kHz and 100 kHz.

The sum of responses can be observed in the simulation in Fig. 3, where in each rise and fall of input square wave, the system behavior presents inverted signal. Consequently, the result is an overlap of responses added by a constant value a referring to variation of the

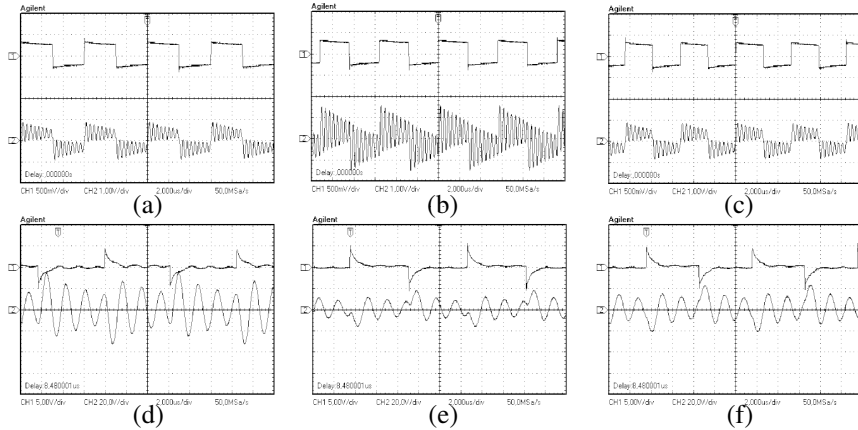


Figure 2. Sum of responses with increasing frequency for configurations 200 turns planar coil *vs* 30 turns ring coil (direct system): (a) 167 kHz; (b) 178 kHz; (c) 191 kHz and 15 turns ring coil *vs* 500 turns planar coil (inverted system): (d) 80 kHz; (e) 90 kHz; (f) 100 kHz.

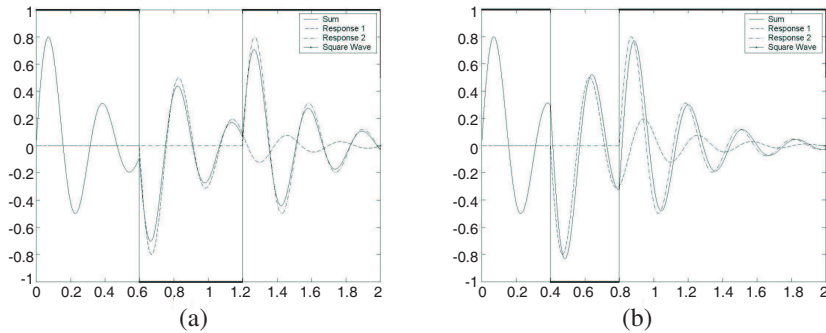


Figure 3. Simulation showing sum of responses in some rise and fall of a square wave.

input. As the input square wave frequency is increased, the peak voltage varies due to this sum. Accordingly [39] this sum of responses is given by:

$$v_0 = \sum_{p=0}^n (-1)^p \left(\alpha \sin(\omega_1(t-p)) e^{-b(t-p)} + a \right) \quad (3)$$

where we see in Fig. 4 the system output voltage in some configurations for direct and inverted systems. In this equation, a is the initial constant value of the response (medium value of the sine wave in initial response), and α is the peak value of the higher frequency of the sine wave response. Thus, the maximum peak to peak voltage is given by:

$$v_{pp\max} = 2 \sum_{i=0}^k \left(\alpha e^{-b\left(\frac{T(4i+1)}{4}\right)} + (-1)^i a \right) \quad (4)$$

where k is the number of cycles of the attenuated oscillatory response of the system, and T is the period of this sine wave ($T = 1/f_{n>} = 2\pi/\omega_1$, where $f_{n>} = \omega_1/2\pi$ is the higher frequency of the response, as shown in [33]). Maximum peak voltage is seen in the simulation shown in Fig. 5, which occurs when $f_s = f_r$, f_s being the frequency of the input square wave and f_r the higher frequency of the sine wave response [38].

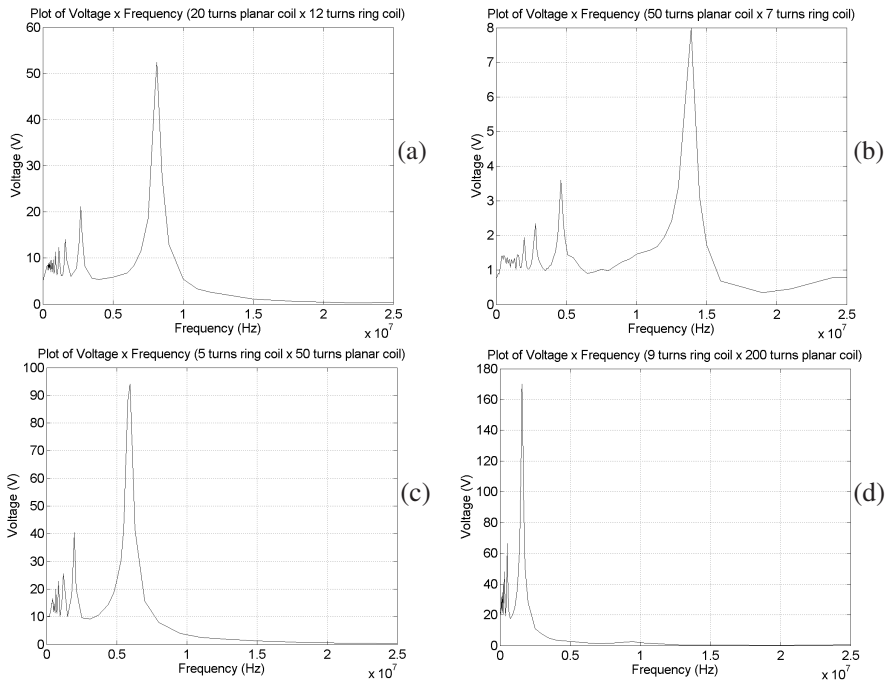


Figure 4. Graphs of frequency *vs* output voltage showing resonance frequency for configurations: (a) 20 turns planar coil *vs* 12 turns ring coil; (b) 50 turns planar coil *vs* 7 turns ring coil; (c) 5 turns ring coil *vs* 50 turns planar coil; (d) 9 turns ring coil *vs* 200 turns planar coil.

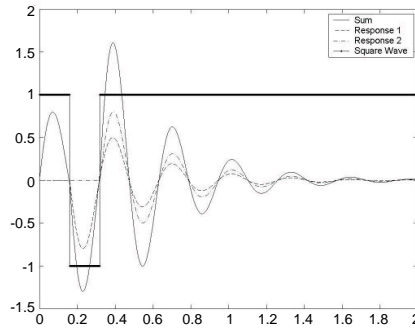


Figure 5. Simulation showing the sum of responses when square wave is in phase with the sinusoidal response.

Analyzing the resonance on system, we see that the output is linear when input voltage is increased. In realized experiments, obtained results show this effect, where ranging input voltage from 1 V to 10 V in resonance frequency, output presents direct proportion. This effect is seen in Figs. 6–8, where some analyzed configurations are shown for comparison (direct and inverted systems).

Other important results can be observed in graphs shown in Fig. 9, where we see resonance output variation when varying turn numbers in ring coil and planar coils for direct system, and in Fig. 10 for inverted system.

In the measurements with 2 turns ring coil in direct system, we observe that the resonance frequency is higher than 25 MHz — limit of the function generator used (which is observed in direct system gain in Figs. 6–8 for configurations involving ring coils with low turn number). This is observed because the peak voltages follow the same graphs for turn numbers greater than 2, which is seen in [39] where resonance frequencies are shifted to higher frequencies when turn number ring coil is decreased. So, when the turn number planar coil increases, resonance frequencies are shifted to lower frequencies. In inverted system, the resonance frequencies are shifted to lower frequencies as it increases the turn number planar coil.

Also, we observe that the greater gain in resonance is found for 5 turn number ring coil, on inverted system, for the experimented coils. In this case, the voltage obtained to 1600 planar coil is 416 V to input voltage of 5 V peak to peak on frequency $f = 407$ kHz, which determines the gain of 83.2 times. However, we observe that due to the sum of responses, in resonance frequency, both direct and inverted systems,

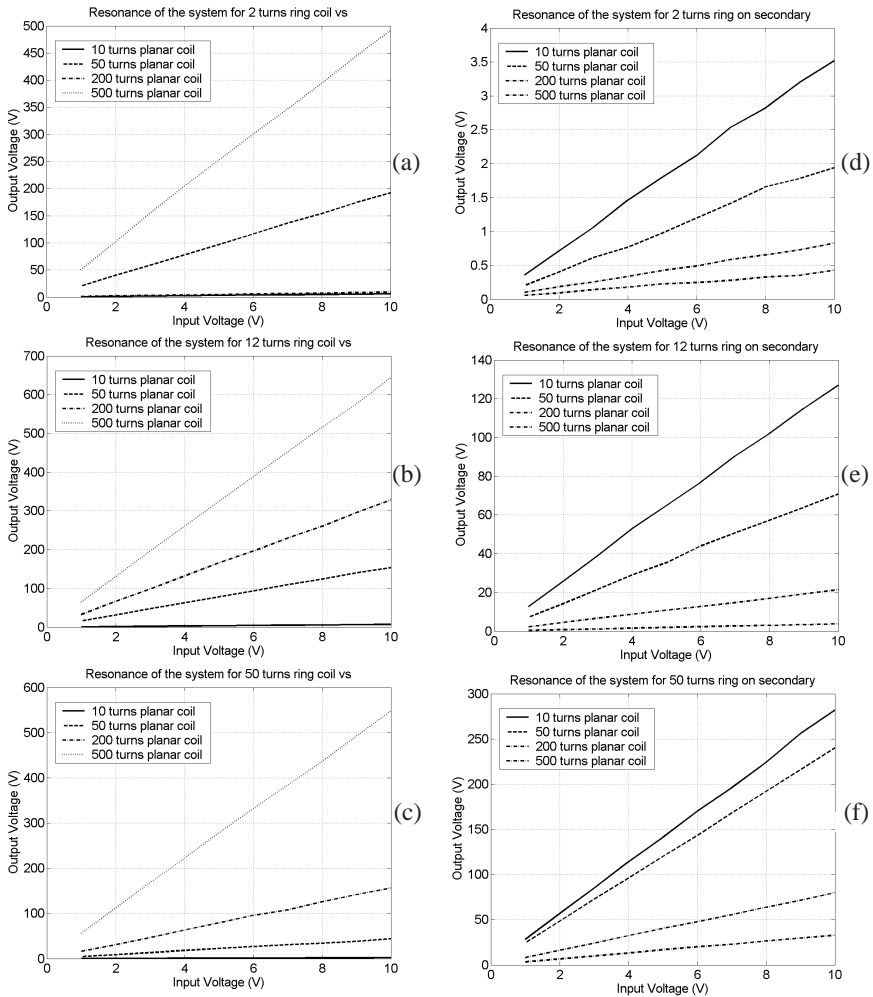


Figure 6. Responses of the system when varying input voltage on system for configurations: (a) 2 turns ring coil; (b) 12 turns ring coil; (c) 50 turns ring coil - *vs* planar coil with 10, 50, 200 and 500 turns (inverted system), and same planar coils *vs* (d) 2 turns ring coil; (e) 12 turns ring coil and (f) 50 turns ring coil (direct system).

the gains are different from that of circuit theory. For example, in configuration 500 turns planar coil *vs* 50 turns ring coil (direct system) for input voltage of 5 V peak to peak, turn ratio is $50/500 = 0.1$, and the output should be 0.5 V peak to peak. But, the sum of responses

generates an output voltage of 16.8 V (gain $16.8/5 = 3.36$) which determines value of $3.36/0.1 = 33.6$ times the theoretical value. For configuration 1600 planar coil *vs* 5 turns ring coil (inverted system), the turn ratio is $1600/5 = 320$, and the expected output voltage is $5 \times 320 = 1560$ V. We obtain $83.2/320 = 0.26$ times theoretical value. This result can be observed analyzing all configurations. Also, we see that gain in resonance to inverted system is lower than theoretical gain due to higher parameters on secondary, which implies lower resonance frequencies and fewer overlapping responses.

These results are found in the systems without parallel capacitances on secondary. The results of the systems with parallel capacitance on output are presented in the next section.

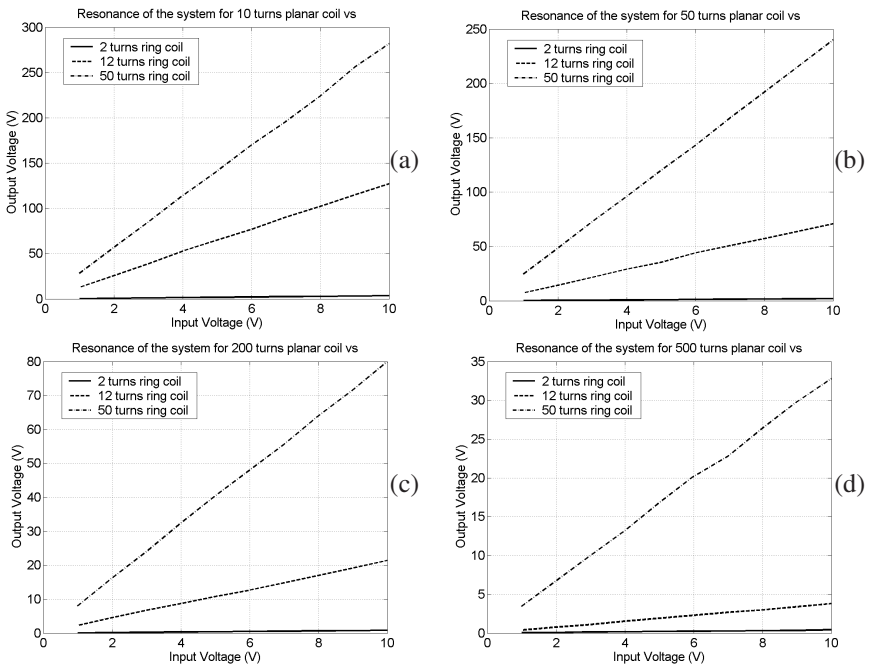


Figure 7. Responses for direct system when varying input voltage for configurations: ring coils with 2, 12 and 50 turns on secondary *vs* (a) 10 turns planar coil; (b) 50 turns planar coil; (c) 200 turns planar coil and (d) 500 turns planar coil.

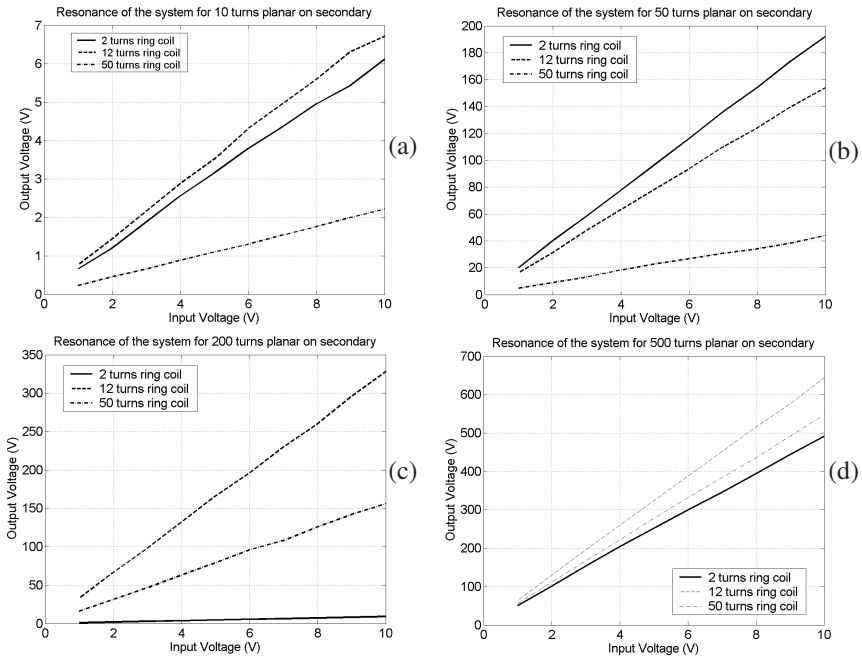


Figure 8. Responses for inverted system when varying input voltage for configurations: ring coils with 2, 12 and 50 turns *vs* (a) 10 turns planar coil; (b) 50 turns planar coil; (c) 200 turns planar coil and (d) 500 turns planar coil.

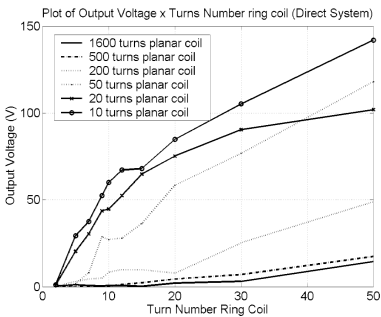


Figure 9. Variation of output voltage in direct system when we change turn number of ring coil for the several planar coils used on experiments.

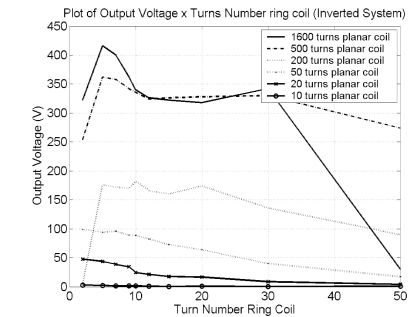


Figure 10. Variation of output voltage in inverted system when we change turn number of ring coil for planar coils used in the experiments.

4. SYSTEM WITH PARALLEL CAPACITANCE IN OUTPUT

The obtained results on previous section were based on measures in the system only with the coils, where effects show the existence of parasitic capacitances [33]. However, these results show how the system reaches output values with high voltages when resonance is reached, which is verified when $f_s = f_r$ [39]. Thus, since we observe these phenomena considering only the coils with their parasitic capacitances, an analysis about inclusion of external capacitances on output is necessary.

The external capacitances included (cited in Section 2) in system were inserted parallel with output, to verify changes on system responses.

Each capacitance was inserted parallel with secondary coil on resonance frequency and observed the changes in response. In all cases, the insertion of parallel capacitances shifted the resonance frequency to lower frequencies. This effect is expected, since the resonance frequency presents relationship with $1/\sqrt{LC}$. Thus, increasing C decreases f , and decreasing f reduces gain. For configurations: 9 turns ring coil *vs* 200 and 500 turns planar coil, we see in Fig. 11 the effects of parallel capacitances inserted in output, considering that the system was tuned in the new resonance frequency, where the first point is the system without parallel capacitance. All measurements were made

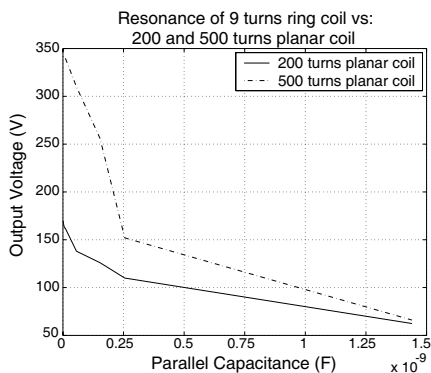


Figure 11. Effect of parallel capacitances inserted in secondary on resonance frequencies for configurations: 9 turns ring coil *vs* 200 and 500 turns planar coil.

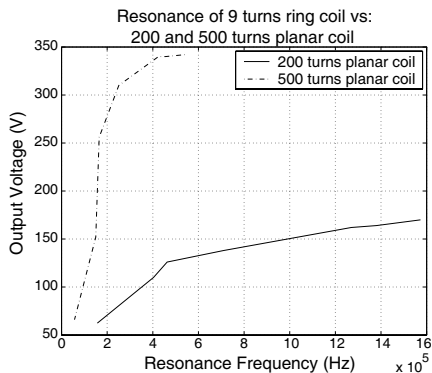


Figure 12. Variation of output voltage due to changes on resonance frequency determined by parallel capacitances value: configurations 9 turns ring coil *vs* 200 and 500 turns planar coils.

with input voltage of 5 V peak to peak. In Fig. 12 the output changes with resonance frequency is observed, where the reached higher value is output voltage of the system without parallel capacitance.

On the other hand, due to insertion of parallel capacitances, changes in gain is too verified. The lower is the parallel capacitance, the higher is the gain, such that, the greater gain is observed when the system presents only its parasitic capacitances. In Fig. 13, we see that the output changes with increasing capacitance.

In all analyzed systems, when varying input voltage from 1 V

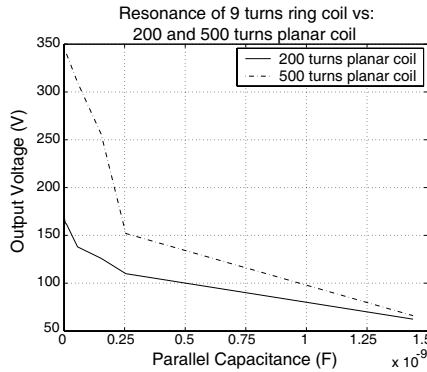


Figure 13. Effect of parallel capacitances inserted in secondary on output voltage for configurations: 9 turns ring coil *vs* 200 and 500 turns planar coil.

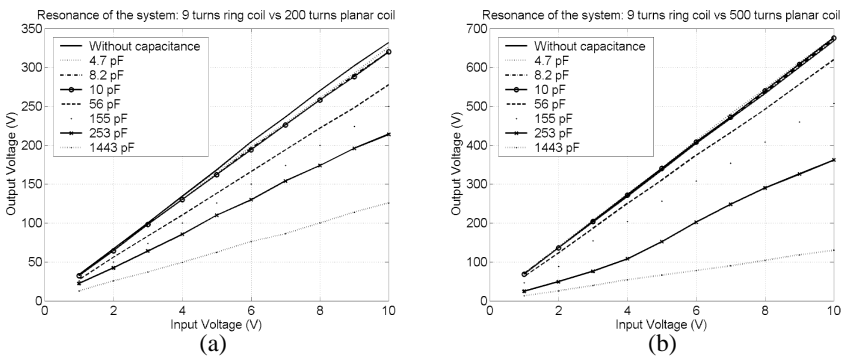


Figure 14. Variation on input voltage and effects of parallel capacitances inserted in secondary for configurations: 9 turns ring coil *vs* 200 and 500 turns planar coil.

to 10 V the gain is maintained. In Fig. 14, we see this effect for configurations: 9 turns ring coil *vs* 200 and 500 turns planar coil, without parallel capacitance and inserting the parallel capacitances.

As shown in Figs. 6–8, the direct system has lower gain than inverted system, but these linearities are equally observed.

In all cases, we observe that the sum of system responses is verified. The linearity of the gain with input voltage is observed too. Also, we observe that the smaller is the capacitance of the system, the higher is the resonance frequency, and the lower is the exponential drop, the greater is the sum of responses. In these experiments, we observe these results, and we see that if parasitic capacitances on system are reduced, satisfying the better relationship with primary of the system (about 5 turns on ring coil) the gain will be better. Due to these results, we can generate comparisons with Tesla transformer and formalize how its phenomenon of high output voltage occurs.

5. TESLA TRANSFORMER AND COMPARISONS WITH OBTAINED RESULTS

Tesla transformer [29–32] is a pulse transformer [23–26] that generates output voltages above 500 kV. This transformer uses an input voltage above 10 kV, applied to a primary coil of low turn number, and generates high voltages on secondary coil built with high turn number. Usually, in basic applications, Tesla transformer consists in a primary with 4 turn number and a secondary with 2000 turn number (coils built as solenoids).

The excitation of the Tesla transformer is made with a pulsed energy generated through a gap which the increased voltage generates the dielectric breakdown of air, exciting primary coil with a pulse of high voltage (running as a rise of a square wave). When the source reduces this value, the pulse on primary is eliminated (the energy is not sufficient for air ionization and the dielectric breakdown of air is eliminated) running as fall of a square wave. Thus, the excitation of Tesla transformer is pulsed, like a square wave, with high voltage.

Considering the experiments worked and presented in this paper, we see that the phenomenon of output high energy of Tesla transformer can be analyzed in a similar way. Since the results of the experiments show that there is a sum of responses in each rise and fall of the square wave, until the resonance ($f_s = f_r$) [39], the same effect is present in Tesla transformer. We see that, as shown in the analyzed systems, parasitic capacitances guarantee the induced *emf* with sinusoidal responses. Considering effects of parallel capacitances inserted in output, the resonance frequency is reduced. The lower the value of

this parallel capacitance, the higher is the resonance frequency and the gain, as seen in Eq. (4).

Also, we observe in obtained results that the best configuration is presented when turn number of primary is low (5 turns, which is approximately the turn number used on basic Tesla transformer) in relationship with the secondary. This fact determines low parasitic capacitances on input, which improves the responses on amplitude of induced *emf* and consequently improves the amplitude of sinusoidal response on output, as shown in [33,38]. Although the realized experiments have been conducted with planar coils, the effects of secondary in Tesla transformer are the same. In the case of the realized experiments and used coils, only the parasitic capacitances present as higher than the parasitic capacitances of the coils on Tesla transformer, as well as the self and mutual inductances.

In Tesla transformer, a parallel capacitor of low capacitance is inserted to improve the output voltage on resonance (which appears in common cases approximately on 400 kHz). Since the sum of responses generates large gains on resonance and considering that the constants α and a in Eq. (4) that depend on the magnetic flux generated by energy on primary coil, these values greatly increase with the input on Tesla transformer. Thus, due to this sum of responses, the high energy on output Tesla transformer in resonance is explained. Although the results of the experiments shown for inverted system (case of Tesla transformer) had presented lower gain than direct system, we see that this problem is due to the parasitic capacitances, self and mutual inductances. In Tesla transformer coils, due to their dimensions, these parameters are much smaller than worked systems.

Moreover, due to results of this paper, improvements on Tesla transformer can be implemented to generate better gain and maximum peak of energy. The ideal for this problem is to generate a higher frequency with less attenuation in the response, such that the input square wave frequency to obtain resonance becomes large, and a greater number of sinusoidal responses with low attenuation is added. In other words, adjustments in parameters of the coils (vary parasitic capacitances, self and mutual inductances, and turn number or wire material to reduces resistances) should be performed to improve the gain. This is currently being researched.

6. CONCLUSIONS

The results presented in this paper are of great importance in several researches of physics and electrical engineering. Effects of resonance on systems excited with square wave can be used in several ways, specially

pulse transformers, power electronics, etc. The results were formalized through experimental works on transformers built with planar coils inner ring coils, exciting primary by square wave with frequencies ranging from 1 kHz to 25 MHz.

The response of induced *emf* in these systems was shown, and the found sum of responses when increasing square wave frequency guarantees the results specially for phenomenon of high energy of the Tesla transformer. We observe that in the resonance frequency, the system gain is determined by the sum of responses, and theoretical gain due to turn ratio is not valid.

The analysis of external capacitances shows reduction of resonance frequency and changes gain due to the sum of responses. We can see that the higher is the parallel capacitances in output, the lower is the gain in resonance and the resonance frequency. In this way, the results to reach better and maximum energy on output of system, as Tesla transformer, should follow these analysis.

The high energy on output of Tesla transformer is the effect of the sum of responses in each rise and fall of the pulse excitation on primary, similar to the results presented in this paper. Also, in accordance to our results, the output Tesla transformer can be improved if the correct values of parameters (self-inductances, resistances, mutual inductance, parasitic capacitances, frequency of the input pulse excitation) are set to obtain high frequency response for the input step voltage (rise and fall of the input pulse) with small exponential drop and maximum value to parameters α and a (Eq. (4)) that is the result of the change in magnetic flux in primary (due to input pulse excitation). Yet, in Tesla transformer the parasitic capacitances, self and mutual inductances, resistances of the coils (due to their dimensions, separation between turns, and diameters of the wires), and parallel output capacitance present lower values than the analyzed systems, which ensures no occurrence of lower gain as observed in some analyzed inverted systems (that is the case of Tesla transformer, where primary has a small turn number and secondary has large turn number). These are the main results of this work.

Moreover, analyzing the results of resonance frequency as feasible effects in circuits, other researches can be realized, applied to power electronics and others applying pulse excitation.

REFERENCES

1. Xiong, J. and L. He, "Extended global routing with RLC crosstalk constraints," *IEEE Transactions on Very Large Scale Integration (VLSI) Systems*, Vol. 13, No. 3, 319–329, March 2005.

2. Ding, W. and G. Wang, "Efficient timing modelling of coupled inductance dominant RLC interconnects," *Electronic Letters*, Vol. 45, No. 1, January 2009.
3. Kim, S. Y. and S. S. Wong, "Closed-form RC and RLC delay models considering input rise time," *IEEE Transactions on Circuits and Systems: Regular Papers*, Vol. 54, No. 9, 2001–2010, September 2007.
4. Agarwal, K., D. Sylvester, and D. Blaauw, "Modeling and analysis of crosstalk noise in coupled RLC interconnects," *IEEE Transactions on Computer-aided Design of Integrated Circuits and Systems*, Vol. 25, No. 5, 892–901, May 2006.
5. Chakravarty, T., S. M. Roy, S. K. Sanyal, and A. De, "Loaded microstrip disk resonator exhibits ultra-low frequency resonance," *Progress In Electromagnetics Research*, PIER 50, 1–12, 2005.
6. Psarros, I. and I. D. Chremmos, "Resonance splitting in two coupled circular closed-loop arrays and investigation of analogy to traveling-wave optical resonators," *Progress In Electromagnetics Research*, PIER 87, 197–214, 2008.
7. Yagashi, A., "Highly improved performance of a noise isolation transformer by a thin-film short circuit ring," *IEEE Transactions on Electromagnetic Compatibility*, Vol. 41, No. 3, 246–250, August 1999.
8. Oshiro, O., H. Tsujimoto, and K. Shirae, "Structures and characteristics of planar transformers," *IEEE Translation Journal on Magnetics in Japan*, Vol. 4, No. 5, 332–338, May 1989.
9. Rissing, L. H., S. A. Zielke, and H. H. Gatzel, "Inductive microtransformer exploiting the magnetoelastic effect," *IEEE Transactions on Magnetics*, Vol. 34, No. 4, 1378–1380, July 1998.
10. Castaldi, G., V. Fiumara, and I. Gallina, "An exact synthesis method for dual-band Chebyshev impedance transformers," *Progress In Electromagnetics Research*, PIER 86, 305–319, 2008.
11. Lu, J. and F. Dawson, "Analysis of eddy current distribution in high frequency coaxial transformer with faraday shield," *IEEE Transactions on Magnetics*, Vol. 42, No. 10, 3186–3188, October 2006.
12. Stadler, A. and M. Albach, "The influence of the winding layout on the core losses and the leakage inductance in high frequency transformers," *IEEE Transactions on Magnetics*, Vol. 42, No. 4, 735–738, April 2006.
13. Cheng, K. W. E., et al., "Examination of square-wave modulated voltage dip restorer and its harmonics analysis," *IEEE*

- Transactions on Energy Conversion*, Vol. 21, No. 3, 759–766, September 2006.
14. Bortis, D., S. Waffler, J. Biela, and J. W. Kolar, “25-kW three-phase unity power factor buckboost rectifier with wide input and output range for pulse load applications,” *IEEE Transactions on Plasma Sciences*, Vol. 36, No. 5, 2747–2752, October 2008.
 15. Evans, P. D. and M. R. D. Al-Mothafar, “Harmonic analysis of a high frequency square wave cycloconverter system,” *IEE Proceedings B*, Vol. 136, No. 1, 19–31, January 1989.
 16. Huang, Z., Y. Cui, and W. Xu, “Application of modal sensitivity for power system harmonic resonance analysis,” *IEEE Transactions on Power Systems*, Vol. 22, No. 1, 222–231, February 2007.
 17. Popov, A. V. and V. V. Kopeikin, “Electromagnetic pulse propagation over nonuniform earth surface: Numerical simulation,” *Progress In Electromagnetics Research B*, Vol. 6, 37–64, 2008.
 18. Qi, J. and A. H. Sihvola, “Truncation effect on precursor field structure of pulse propagation in dispersive media,” *Progress In Electromagnetics Research B*, Vol. 14, 65–86, 2009.
 19. Butrym, A. Y. and M. N. Legenkiy, “Charge transport by a pulse E-wave in a waveguide with conductive medium,” *Progress In Electromagnetics Research B*, Vol. 15, 325–346, 2009.
 20. Hussain, M. G. M. and S. F. Mahmoud, “Energy patterns for a conducting circular disc buried in a homogeneous lossy medium and excited by ultra-wideband generalized gaussian pulses,” *Progress In Electromagnetics Research*, PIER 43, 59–74, 2003.
 21. Besieris, I., M. Abdel-Rahman, A. Shaarawi, and A. Chatzipetros, “Two fundamental representations of localized pulse solution to the scalar wave equation,” *Progress In Electromagnetics Research*, PIER 19, 1–48, 1998.
 22. Ala, G., M. L. D. Silvestre, F. Viola, and E. Francomano, “Soil ionization due to high pulse transient currents leaked by earth electrodes,” *Progress In Electromagnetics Research B*, Vol. 14, 1–21, 2009.
 23. Lord, H. W., “Pulse transformers,” *IEEE Transactions on Magnetics*, Vol. 7, No. 1, 17–28, March 1971.
 24. Redondo, L. M., J. F. Silva, and E. Margato, “Pulse shape improvement in core-type high-voltage pulse transformers with auxiliary windings,” *IEEE Transactions on Magnetics*, Vol. 43, No. 5, 1973–1982, May 2007.
 25. Brown, D. and D. Martin, “Subnanosecond high-voltage pulse

- generator,” *Rev. Sci. Instrum.*, Vol. 58, No. 8, 1523–1529, August 1987.
26. Luthjens, L. H., M. L. Hom, and M. J. W. Vermeulen, “Subnanosecond pulsing of a 3-MV Van de Graaff electron accelerator by means of a passive coaxial pulse shaper,” *Rev. Sci. Instrum.*, Vol. 49, No. 2, 230–235, February 1978.
 27. Riabi, M. L., R. Thabet, and M. Belmeguenai, “Rigorous design and efficient optimization of quarter-wave transformers in metallic circular waveguides using the mode-matching method and the genetic algorithm,” *Progress In Electromagnetics Research*, PIER 68, 15–33, 2007.
 28. Wu, Y., Y. Liu, and S. Li, “A compact pi-structure dual band transformer,” *Progress In Electromagnetics Research*, PIER 88, 121–134, 2008.
 29. Dinev, D. K., “Design of Tesla transformers used in direct-voltage accelerators,” *Atomic Energy*, Vol. 46, No. 3, March 1979.
 30. Jain, K. K., D. Chennareddy, P. I. John, and Y. C. Saxena, “Design and performance of a Tesla transformer type relativistic electron beam generator,” *Sadhana*, Vol. 9, No. 1, February 1986.
 31. Korovin, S. D. and V. V. Rostov, “High-current nanosecond pulse-periodic electron accelerators utilizing a Tesla transformer,” *Russian Physics Journal*, Vol. 39, No. 12, December 1996.
 32. Ying, P. and R. Jiangjun, “Investigation of very fast transient overvoltage distribution in taper winding of tesla transformer,” *IEEE Transactions on Magnetics*, Vol. 42, No. 3, 434–441, March 2006.
 33. Costa, E. M. M., “A basic analysis about induced EMF of planar coils to ring coils,” *Progress In Electromagnetic Research B*, Vol. 17, 85–100, August 2009.
 34. Grandi, G., et al., “Stray capacitances of single-layer solenoid air-core inductors,” *IEEE Transactions on Industry Applications*, Vol. 35, No. 5, 1162–1168, September/October 1999.
 35. Hole, M. J. and L. C. Appel, “Stray capacitance of a two-layer air-cored inductor,” *IEE Proc. — Circuits Devices Syst.*, Vol. 152, No. 6, 565–572, December 2005.
 36. Marin, D., et al., “Modelling parasitic capacitances of the isolation transformer,” *In. Simpozionul National de Eletrotehnica Teoretica, SNET 2004*, Bucharest, October 2004.
 37. Kamarudin, M. R. and P. S. Hall, “Switched beam antenna array with parasitic elements,” *Progress In Electromagnetics Research B*, Vol. 13, 187–201, 2009.

38. Costa, E. M. M., "Responses in transformers built with planar coils inner ring coils excited by square waves," *Progress In Electromagnetic Research B*, Vol. 18, 43–58, September 2009.
39. Costa, E. M. M., "Resonance between planar coils vs ring coils excited by square waves," *Progress In Electromagnetic Research B*, Vol. 18, 59–81, September 2009.
40. Kaware, K., H. Kotama, and K. Shirae, "Planar inductor," *IEEE Transactions on Magnetics*, Vol. 20, No. 5, 1984–1806, September 1984.
41. Babic, S. I. and C. Akyel, "Improvement in calculation of the self- and mutual inductance of thin-wall solenoids and disk coils," *IEEE Transactions on Magnetics*, Vol. 36, No. 4, 1970–1975, July 2000.
42. Matsuki, H., N. Fujii, K. Shirakawa, J. Toriu, and K. Murakami, "Planar coil inductor with closed magnetic circuit," *IEEE Translation Journal on Magnetics in Japan*, Vol. 7, No. 6, 474–478, June 1992.
43. Babic, S. I., S. Kincic, and C. Akyel, "New and fast procedures for calculating the mutual inductance of coaxial circular coils (circular coildisk coil)," *IEEE Transactions on Magnetics*, Vol. 38, No. 5, 2367–2369, September 2002.
44. Su, Y. P., X. Liu, and S. Y. R. Hui, "Mutual inductance calculation of movable planar coils on parallel surfaces," *IEEE Transactions on Power Electronics*, Vol. 24, No. 4, 1115–1124, April 2009.
45. Oshiro, O., H. Tsujimoto, and K. Shirae, "A novel miniature planar inductor," *IEEE Transactions on Magnetics*, Vol. 23, No. 5, 3759–3761, September 1987.
46. Anioin, B. A., et al., "Circuit properties of coils," *IEE Proc. — Sci. Mes. Technol.*, Vol. 144, No. 5, 234–239, September 1997.
47. Asdler, M. S., "A field-theoretical approach to magnetic induction of thin circular plates," *IEEE Transactions on Magnetics*, Vol. 10, No. 4, 1118–1125, December 1974.
48. Dudek, C., et al., "A new type of highly compact planar inductor," *IEEE Transactions on Magnetics*, Vol. 43, No. 6, 2621–2623, June 2007.
49. Kim, Y., F. Yang, and A. Z. Elsherbeni, "Compact artificial magnetic conductor desings using planar square spiral geometries," *Progress In Electromagnetics Research*, PIER 77, 43–54, 2007.
50. Conway, J. T., "Noncoaxial inductance calculations without the vector potential for axissymmetric coils and planar coils," *IEEE Transactions on Magnetics*, Vol. 44, No. 4, 453–462, April 2008.

51. Hurley, W. G. and M. C. Duffy, "Calculation of self- and mutual impedances in planar sandwich inductors," *IEEE Transactions on Magnetics*, Vol. 33, No. 3, 2282–2290, May 1997.